Supporting Information

n-Type Organic Field-Effect Transistors Based on Bisthienoisatin Derivatives

Dongho Yoo,[*,†] *Xuyi Luo,*[‡] *Tsukasa Hasegawa,*[†] *Minoru Ashizawa,*[*,†] *Tadashi Kawamoto,*[†] *Hiroyasu Masunaga,*[§] *Noboru Ohta,*[§] *Hidetoshi Matsumoto,*[†] *Jianguo Mei,*[‡] *and Takehiko Mori**[*,†]

[†] Department of Materials Science and Engineering, Tokyo Institute of Technology, O-okayama 2-12-1, Meguro-ku, Tokyo 152-8552, Japan.

[‡] Department of Chemistry, Purdue University, West Lafayette, Indiana 47907, United States.

[§] Japan Synchrotron Radiation Research Institute (JASRI/SPring-8), 1-1-1 Kouto, Sayo-cho, Sayo-gun, Hyogo 679-5198, Japan.

Corresponding Author

* E-mail: yoo.d.aa@m.titech.ac.jp, ashizawa.m.aa@m.titech.ac.jp, mori.t.ae@m.titech.ac.jp

Downloaded from pubs.acs.org/aaembp/article-supplement/617211/pdf/el9b00105_si_001/ by PURDUE UNIV user on 28 October 2026

I. General

Commercially available materials were used as received. Anhydrous solvents (DCM, DMSO, and EtOH) were purchased from Wako Pure Chemical Industries. All reactions were conducted under argon atmosphere. For thin-layer chromatography (TLC) analysis, Merck pre-coated glass plates (TLC Silica gel 60 F254) were used. Silica gel used in chromatographic separations was obtained from Wako Pure Chemical Industries (Wako Silica Gel C-200 (spherical, neutral), 75−150 μm). ^{1}H NMR (300 MHz) spectra were obtained with a JEOL JNM-AL300 spectrometer with $CDCl_3$ as a solvent using Me_4Si as an internal standard. EI-Mass spectra were obtained on a JEOL JMS-Q1050GC Ultra Quad GC/MS spectrometer. Elemental analyses were performed at the Center for Advanced Materials Analysis, Tokyo Institute of Technology.

Downloaded from pubs.acs.org/aaembp/article-supplement/617211/pdf/el9b00105_si_001/ by PURDUE UNIV user on 28 October 2026

II. Synthesis

1a-c were synthesized with an Ullmann coupling of 3-bromothiophene and *R*-amine.[S1]

***N*-propylthiophen-3-amine (1a)**

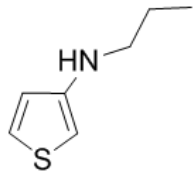

3-Bromothiophene (8.15 g, 50 mmol) was dissolved in *N*,*N*-dimethylaminoethanol (30 mL) under an argon atmosphere. To the resulting solution, copper (0.19 g, 3 mmol), copper(I) iodide (0.57 g, 3 mmol), potassium phosphate tribasic (31.8 g, 150 mmol) and propylamine (4.5 g, 75 mmol) were added successively, and the mixture was stirred at 45°C for 72 h. After the reaction mixture was allowed to cool to room temperature, the mixture was filtered. The residue was washed with dichloromethane and the filtrate was concentrated and subjected to silica column chromatography eluted with hexane-dichloromethnae (9/1 = v/v) to afford **1a** (3.15 g, 22.3 mmol, yield 45.0%) as a yellow air sensitive liquid. EI-MS *m*/*z*: 141 $[M]^+$. ^{1}H NMR (300 MHz, $CDCl_3$, 25°C): δ 7.09 (dd, J = 5.1 Hz, 3.3 Hz, 1H), 6.56 (dd, J = 5.1 Hz, 1.5 Hz, 1H), 5.80 (dd, J = 2.9 Hz, 1.5 Hz, 1H), 3.51 (s, 1H), 3.00 (t, J = 7.0 Hz, 2H), 1.67-1.57 (m, 2H), 0.97 (t, J = 7.5 Hz, 3H). ^{13}C NMR (75 MHz, $CDCl_3$, 25°C): δ 148.77, 124.83, 119.78, 95.07, 48.09, 22.68, 11.54.

Downloaded from pubs.acs.org/aaembp/article-supplement/617211/pdf/el9b00105_si_001/ by PURDUE UNIV user on 28 October 2026

***N*-hexylthiophen-3-amine (1b)**

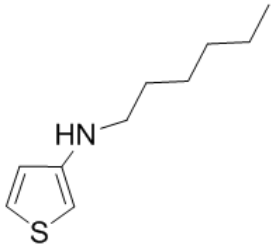

1b (yield 43.0%) was prepared according to the previous report.[S2]

***N*-(2-ethylhexyl)thiophen-3-amine (1c)**

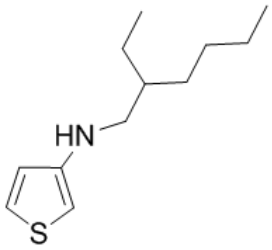

3-Bromothiophene (8.15 g, 50 mmol) was dissolved in *N*,*N*-dimethylaminoethanol (30 mL) under an argon atmosphere. To the resulting solution, copper (0.19 g, 3 mmol), copper(i) iodide (0.57 g, 3 mmol), potassium phosphate tribasic (31.8 g, 150 mmol) and 2-ethylhexylamine (9.7 g, 75 mmol) were added successively, and the mixture was stirred at 90°C for 48 h. After the reaction mixture was allowed to cool to room temperature, the mixture was filtered. The residue was washed with dichloromethane and the filtrate was concentrated and subjected to silica column chromatography eluted with hexane-dichloromethnae (4/1 = v/v) to afford **1c** (3.36 g, 15.9 mmol, yield 31.8%) as a yellow air sensitive liquid. EI-MS *m*/*z*: 211 $[M]^+$. ^{1}H NMR (300 MHz, $CDCl_3$, 25°C): δ 7.15 (d, J = 4.9 Hz, 1H), 6.62 (d, J = 4.9 Hz, 1H), 5.93 (s, 1H), 3.58 (br s, 1H), 3.01 (d, J = 6.2 Hz, 2H), 1.59-1.55 (m, 1H), 1.43-1.37 (m, 8H), 0.96-0.94 (m, 6H). ^{13}C NMR (75 MHz, $CDCl_3$, 25°C): δ 149.17, 124.96, 119.96, 94.81, 49.54, 39.31, 31.48, 29.12, 24.64, 23.16, 14.14, 11.02.

Downloaded from pubs.acs.org/aaembp/article-supplement/617211/pdf/el9b00105_si_001/ by PURDUE UNIV user on 28 October 2026

4-propyl-4H-thieno[3,2-b]pyrrole-5,6-dione (**2a**)

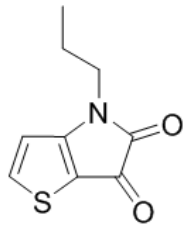

A solution of oxalyl chloride (4.25 g, 33.5 mmol) in anhydrous dichloromethane (20 mL) was cooled to 0°C under an argon atmosphere. A solution of **1a** (3.15 g, 22.3 mmol) dissolved in anhydrous dichloromethane (20 mL) was dropwise added over 30 min. After 30 min, a solution of trimethylamine (6.80 g, 67.2 mmol) in anhydrous dichloromethane (20 mL) was dropwise added over 1 h. The resulting mixture was allowed to warm to room temperature. After stirring for 12 h at room temperature, the mixture was quenched with water, and the organic layer was extracted with dichloromethane and washed with brine and water. The organic layer was dried over $MgSO_4$, and the solvent was removed under reduced pressure. The residue was purified by silica-gel chromatography eluted with hexane-dichloromethane (gradient from 1/1 = v/v to 1/4 = v/v) to afford **2a** (1.36 g, 6.97 mmol, yield 31.3%). EI-MS *m*/*z*: 195 $[M]^+$. ^{1}H NMR (300 MHz, $CDCl_3$, 25°C): δ 8.01 (d, J = 4.8 Hz, 1H), 6.79 (d, J = 4.8 Hz, 1H), 3.61 (t, J = 7.1 Hz, 2H), 1.72-1.65 (m, 2H), 0.94 (t, J = 7.3 Hz, 3H). ^{13}C NMR (75 MHz, $CDCl_3$, 25°C): δ 173.10, 165.35, 161.67, 144.18, 113.16, 111.05, 43.78, 21.61, 11.33.

Downloaded from pubs.acs.org/aaembp/article-supplement/617211/pdf/el9b00105_si_001/ by PURDUE UNIV user on 28 October 2026

4-hexyl-4H-thieno[3,2-b]pyrrole-5,6-dione (**2b**)

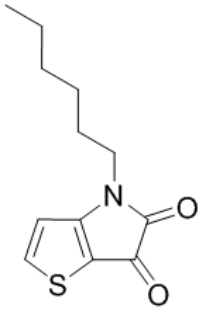

2b (yield 47.1%) was prepared according to the previous report.[S2]

4-(2-ethylhexyl)-4H-thieno[3,2-b]pyrrole-5,6-dione (**2c**)

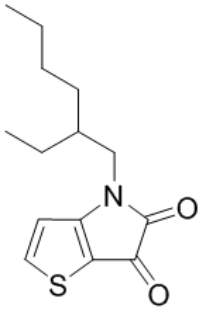

A solution of oxalyl chloride (3.05 g, 24.0 mmol) in anhydrous dichloromethane (20 mL) was cooled to 0°C under an argon atmosphere. A solution of **1c** (3.36 g, 15.9 mmol) dissolved in anhydrous dichloromethane (20 mL) was dropwise added over 30 min. After 30 min, a solution of trimethylamine (4.80 g, 47.4 mmol) in anhydrous dichloromethane (20 mL) was dropwise added over 1 h. The resulting mixture was allowed to warm to room temperature. After stirring for 12 h at room temperature, the mixture was quenched with water, and the organic layer was extracted with dichloromethane and washed with brine and water. The organic layer was dried over $MgSO_4$, and the solvent was removed under reduced pressure. The residue was purified by silica-gel chromatography eluted with hexane-dichloromethane (gradient from 1/1 = v/v to 1/4 = v/v) to afford **2c** (1.20 g, 4.52 mmol, yield 28.4%). EI-MS *m*/*z*: 265 $[M]^+$. ^{1}H NMR (300 MHz,

Downloaded from pubs.acs.org/aaembp/article-supplement/617211/pdf/el9b00105_si_001/ by PURDUE UNIV user on 28 October 2026

$CDCl_3$, 25°C): δ 8.01 (d, J = 5.5 Hz, 1H), 6.78 (d, J = 5.5 Hz, 1H), 3.54 (d, J = 7.0 Hz, 2H), 1.74 (t, J = 6.0 Hz, 1H), 1.36-1.32 (m, 8H), 0.93-0.89 (m, 6H). ^{13}C NMR (75 MHz, $CDCl_3$, 25°C): δ 173.02, 165.55, 161.81, 143.86, 113.20, 111.11, 46.13, 38.34, 30.53, 28.61, 23.89, 22.99, 14.02, 10.55.

4,4'-dipropyl-4H,4'H-[2,2'-bithieno[3,2-b]pyrrole]-5,5',6,6'-tetraone (BTI-Pr)

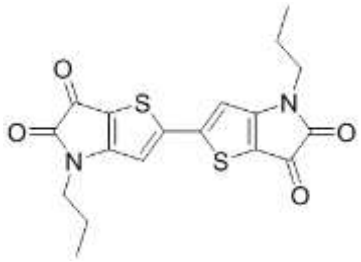

Compound **2a** (1.36 g, 6.97 mmol), silver fluoride (2.22 g, 17.5 mmol) and palladium(II) acetate (0.16 g, 0.713 mmol) were added to 40 mL of anhydrous DMSO under an argon atmosphere. The resulting mixture was heated to 90°C and stirred for 24 h. After cooling to room temperature, the reaction mixture was poured into water, extracted with dichloromethane and the organic layer was washed with water. The organic layer was dried over $MgSO_4$, and the solvent was removed under reduced pressure. The residue was purified by silica-gel chromatography eluted with dichloromethane-ethyl acetate (gradient from 9/1 = v/v to 1/1 = v/v) to afford **BTI-Pr** (0.19 g, 0.49 mmol, yield 14.1%) as a purple-red solid. EI-MS m/z: 388 $[M]^+$. ^{1}H NMR (300 MHz, $CDCl_3$, 25°C): δ 7.01 (s, 2H), 3.69 (t, J = 7.1 Hz, 4H), 1.79-1.74 (m, 4H), 1.02 (t, J = 7.5 Hz, 6H). ^{13}C NMR (75 MHz, $CDCl_3$, 25°C): δ 172.37, 164.44, 159.79, 151.70, 111.78, 110.77, 44.01, 21.62, 11.26. Anal. Calcd for $C_{18}H_{16}N_2O_4S_2$: C, 55.66; H, 4.15; N, 7.21; O, 16.47; S, 16.51; found: C, 55.44; H, 4.06; N, 7.13; O, 16.32; S, 16.58.

Downloaded from pubs.acs.org/aaembp/article-supplement/617211/pdf/el9b00105_si_001/ by PURDUE UNIV user on 28 October 2026

4,4'-dihexyl-4H,4'H-[2,2'-bithieno[3,2-b]pyrrole]-5,5',6,6'-tetraone (BTI-Hex)

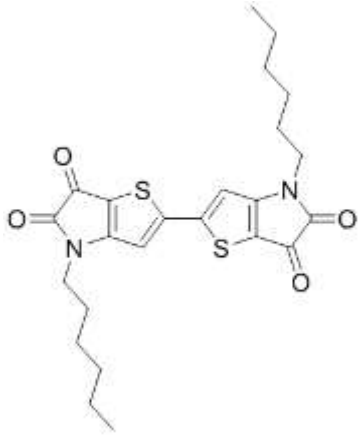

Compound **2b** (1.18 g, 4.97 mmol), silver fluoride (1.39 g, 11.0 mmol) and palladium(II) acetate (0.11 g, 0.490 mmol) were added to 40 mL of anhydrous DMSO under an argon atmosphere. The resulting mixture was heated to 90°C and stirred for 24 h. After cooling to room temperature, the reaction mixture was poured into water, extracted with dichloromethane and the organic layer was washed with water. The organic layer was dried over $MgSO_4$, and the solvent was removed under reduced pressure. The residue was purified by silica-gel chromatography eluted with dichloromethane-ethyl acetate (gradient from 10/0 = v/v to 9/1 = v/v) to afford **BTI-Hex** (0.45 g, 0.95 mmol, yield 38.2%) as a purple-red solid. EI-MS *m*/*z*: 472 $[M]^+$. ^{1}H NMR (300 MHz, $CDCl_3$, 25°C): δ 7.00 (s, 2H), 3.70 (t, J = 7.1 Hz, 4H), 1.71 (t, J = 7.0 Hz, 4H), 1.36-1.32 (m, 12H), 0.90 (t, J = 7.0 Hz, 6H). ^{13}C NMR (75 MHz, $CDCl_3$, 25°C): δ 172.53, 164.52, 160.56, 151.89, 111.73, 110.82, 42.44, 31.39, 28.28, 26.53, 22.60, 14.05. Anal. Calcd for $C_{24}H_{28}N_2O_4S_2$: C, 60.99; H, 5.97; N, 5.93; O, 13.54; S, 13.57; found: C, 60.93; H, 5.73; N, 5.80; O, 13.22.

Downloaded from pubs.acs.org/aaembp/article-supplement/617211/pdf/el9b00105_si_001/ by PURDUE UNIV user on 28 October 2026

4,4'-bis(2-ethylhexyl)-4H,4'H-[2,2'-bithieno[3,2-b]pyrrole]-5,5',6,6'-tetraone (BTI-EH)

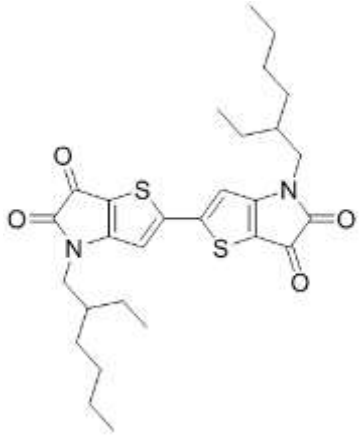

Compound **2c** (1.20 g, 4.52 mmol), silver fluoride (1.40 g, 11.0 mmol) and palladium(II) acetate (0.11 g, 0.490 mmol) were added to 40 mL of anhydrous DMSO under an argon atmosphere. The resulting mixture was heated to 90°C and stirred for 24 h. After cooling to room temperature, the reaction mixture was poured into water, extracted with dichloromethane and the organic layer was washed with water. The organic layer was dried over $MgSO_4$, and the solvent was removed under reduced pressure. The residue was purified by silica-gel chromatography eluted with dichloromethane-ethyl acetate (gradient from 10/0 = v/v to 9/1 = v/v) to afford **BTI-EH** (0.52 g, 0.98 mmol, yield 43.4%) as a purple-red solid. EI-MS *m*/*z*: 528 $[M]^+$. ^{1}H NMR (300 MHz, $CDCl_3$, 25°C): δ 6.94 (s, 2H), 3.58 (d, J = 7.3 Hz, 4H), 1.79-1.76 (m, 2H), 1.35-1.32 (m, 16H), 0.97-0.92 (m, 12H). ^{13}C NMR (75 MHz, $CDCl_3$, 25°C): δ 172.50, 164.81, 160.73, 151.60, 110.85, 46.42, 38.47, 30.58, 28.58, 24.01, 22.97, 13.96, 10.52 (two peaks are overlapped as an one peak). Anal. Calcd for $C_{28}H_{36}N_2O_4S_2$: C, 63.61; H, 6.86; N, 5.30; O, 12.10; S, 12.13; found: C, 63.51; H, 6.95; N, 5.30; O, 12.03; S, 11.94.

Downloaded from pubs.acs.org/aaembp/article-supplement/617211/pdf/el9b00105_si_001/ by PURDUE UNIV user on 28 October 2026

2,2'-(5,5'-dioxo-4,4'-dipropyl-4,4',5,5'-tetrahydro-6H,6'H-[2,2'-bithieno[3,2-b]pyrrole]-6,6'-diylidene)dimalononitrile (**BTICN-Pr**)

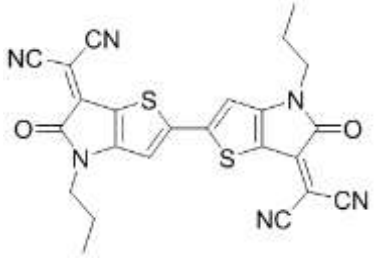

Compound **BTI-Pr** (0.15 g, 0.39 mmol) and malononitrile (0.09 g, 1.36 mmol) were added to anhydrous EtOH (20 mL) under an argon atmosphere. The mixture was heated to reflux. The reaction mixture was stirred until the starting material disappeared completely by thin layer chromatography. After cooling to room temperature, the solvent was removed under reduced pressure. The residue was purified by silica-gel chromatography eluted with dichloromethane-ethyl acetate (gradient from 10/0 = v/v to 9/1 = v/v) to afford **BTICN-Pr** (0.04 g, 0.083 mmol, yield 21.3%) as a purple solid. EI-MS *m*/*z*: 484 $[M]^+$. ^{1}H NMR (300 MHz, $CDCl_3$, 25°C): δ 7.04 (s, 2H), 3.69 (t, J = 7.0 Hz, 4H), 1.75-1.72 (m, 4H), 1.00 (t, J = 3.8 Hz, 6H). Anal. Calcd for $C_{24}H_{16}N_6O_2S_2$: C, 59.49; H, 3.33; N, 17.34; O, 6.60; S, 13.23; found: C, 59.25; H, 3.50; N, 17.26.

Downloaded from pubs.acs.org/aaembp/article-supplement/617211/pdf/el9b00105_si_001/ by PURDUE UNIV user on 28 October 2026

2,2'-(4,4'-dihexyl-5,5'-dioxo-4,4',5,5'-tetrahydro-6H,6'H-[2,2'-bithieno[3,2-b]pyrrole]-6,6'-diylidene)dimalononitrile (**BTICN-Hex**)

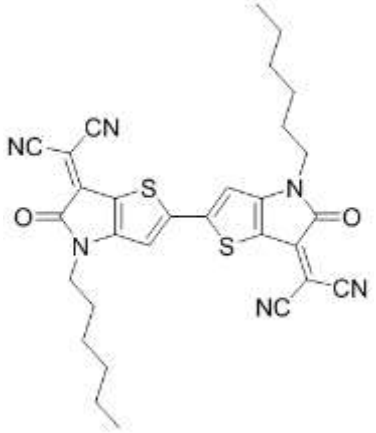

Compound **BTI-Hex** (0.15 g, 0.32 mmol) and malononitrile (0.07 g, 1.06 mmol) were added to anhydrous EtOH (20 mL) under an argon atmosphere. The mixture was heated to reflux. The reaction mixture was stirred until the starting material disappeared completely by thin layer chromatography. After cooling to room temperature, the solvent was removed under reduced pressure. The residue was purified by silica-gel chromatography eluted with dichloromethane to afford **BTICN-Hex** (0.05 g, 0.088 mmol, yield 27.5%) as a purple solid. EI-MS *m*/*z*: 569 $[M]^+$. ^{1}H NMR (300 MHz, $CDCl_3$, 25°C): δ 7.02 (s, 2H), 3.73 (t, J = 7.3 Hz, 4H), 1.72 (t, J = 7.0 Hz, 4H), 1.37-1.34 (m, 12H), 0.91 (t, J = 6.2 Hz, 6H). Anal. Calcd for $C_{30}H_{28}N_6O_2S_2$: C, 63.36; H, 4.96; N, 14.78; O, 5.63; S, 11.27; found: C, 63.05; H, 4.87; N, 14.56; O, 5.92; S, 11.49.

Downloaded from pubs.acs.org/aaembp/article-supplement/617211/pdf/el9b00105_si_001/ by PURDUE UNIV user on 28 October 2026

2,2'-(4,4'-bis(2-ethylhexyl)-5,5'-dioxo-4,4',5,5'-tetrahydro-6H,6'H-[2,2'-bithieno[3,2-b]pyrrole]-6,6'-diylidene)dimalononitrile (BTICN-EH)

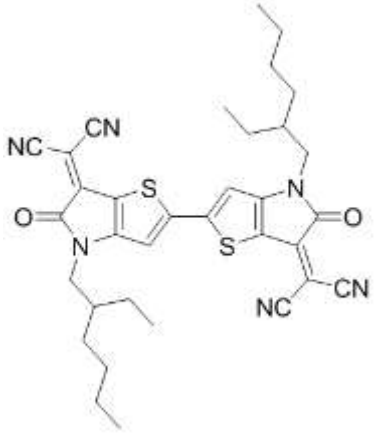

Compound **BTI-EH** (0.15 g, 0.28 mmol) and malononitrile (0.07 g, 1.06 mmol) were added to anhydrous EtOH (20 mL) under an argon atmosphere. The mixture was heated to reflux. The reaction mixture was stirred until the starting material disappeared completely by thin layer chromatography. After cooling to room temperature, the solvent was removed under reduced pressure. The residue was purified by silica-gel chromatography eluted with dichloromethane to afford **BTICN-EH** (0.05 g, 0.080 mmol, yield 28.6%) as a purple solid. EI-MS *m*/*z*: 624 $[M]^+$. ^{1}H NMR (300 MHz, $CDCl_3$, 25°C): δ 6.97 (s, 2H), 3.61 (d, J = 7.7 Hz, 4H), 1.79 (br s, 2H), 1.38-1.33 (m, 16H), 0.97-0.91 (m, 12H). ^{13}C NMR (75 MHz, $CDCl_3$, 25°C): δ 164.44, 158.13, 151.00, 144.45, 115.23, 113.56, 110.67, 109.94, 46.54, 38.32, 30.30, 28.39, 23.71, 23.01, 14.05, 10.39. Anal. Calcd for $C_{34}H_{36}N_6O_2S_2$: C, 65.36; H, 5.81; N, 13.45; O, 5.12; S, 10.26; found: C, 65.08; H, 5.87; N, 13.33; S, 10.11.

Downloaded from pubs.acs.org/aaembp/article-supplement/617211/pdf/el9b00105_si_001/ by PURDUE UNIV user on 28 October 2026

III. Electrochemical properties, optical properties and DFT calculations

Cyclic voltammetry (CV) was carried out using an ALS model 701E electrochemical analyzer. The measurement was performed in a dehydrated dichloromethane (DCM) solution containing 0.1 M tetra-*n*-butylammonium hexafluorophosphate (*n*-$Bu_4N \cdot PF_6$) as a supporting electrolyte using a glassy carbon working electrode, a platinum counter electrode, and an $Ag/AgNO_3$ electrode as a reference electrode at the scan rate of 50 mV s^{-1}. The half−wave potential of ferrocene appeared at 0.197 V from the $Ag/AgNO_3$ reference electrode. The LUMO levels of **BTI**s and **BTICN**s were estimated by assuming the ferrocene/ferrocenium energy level to be −4.8 eV under the vacuum level.[S3]

UV-vis spectra were measured on a Shimadzu Corporation UV-1800 in DCM solutions and for thin films. The absorption spectra of thin films with the thickness of 20 nm thermally deposited on glass substrates are shown in Figure S1. Thin films of **BTI**s show almost the same absorption (Figure S1a). In **BTICN**s, however, **BTICN-EH** shows red-shifted absorption compared to **BTICN-Pr** and **BTICN-Hex** (Figure S1b and Table S1), indicating strong intermolecular interaction in the solid state. This is favorable to the thin-film transistors, so that this may be related to the highest electron mobility of **BTICN-EH** (Table 5).

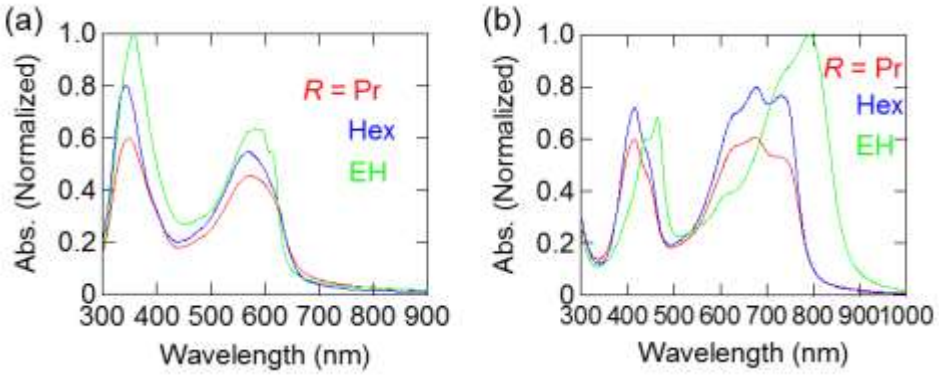

Figure S1. UV-vis absorption spectra of thin films of (a) **BTI**s and (b) **BTICN**s.

Downloaded from pubs.acs.org/aaembp/article-supplement/617211/pdf/el9b00105_si_001/ by PURDUE UNIV user on 28 October 2026

Table S1. Optical properties of thin films.

Compound	Alkyl (*R*)	λ_{onset} (nm)	λ_{max} (nm)	E_g^{opt} (eV)
BTI	Pr	658	347, 571	1.88
	Hex	658	343, 568	1.88
	EH	638	357, 580	1.94
BTICN	Pr	797	414, 675, 726	1.55
	Hex	787	415, 678, 731	1.57
	EH	867	444, 464, 791	1.43

The density functional calculations were performed with the B3LYP* functional and TZP basis set using the ADF software.[36] Methyl groups were attached to the *N*-positions. The electron density distribution maps of the LUMO levels in the neutral **BTI** and **BTICN** are shown in Figure S2. The LUMO levels calculated at the by the B3LYP*/TZP level are −4.08 eV for **BTI** and −4.81 eV for **BTICN**.

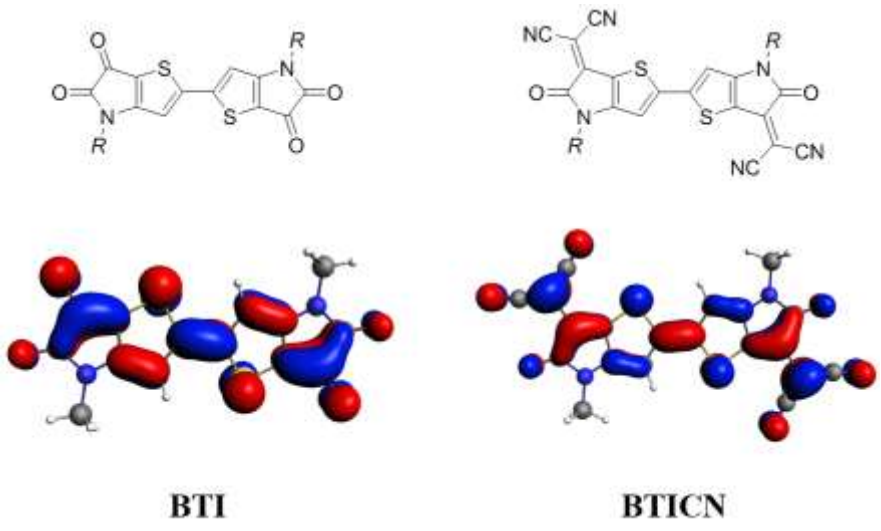

Figure S2. LUMOs of **BTI** and **BTICN** calculated at the by the B3LYP*/TZP level.

Downloaded from pubs.acs.org/aaembp/article-supplement/617211/pdf/el9b00105_si_001/ by PURDUE UNIV user on 28 October 2026

IV. Single crystal X-ray structure analyses

Single crystals of **BTI-Pr** and **BTI-Hex** were obtained from the acetone solutions, and single crystals of **BTICN-Hex** were obtained from the chloroform solution. Single crystals of **BTICN-EH** were obtained by the solvent vapor diffusion of ethanol to the tetrahydrofuran solution. Single-crystal X-ray structure analyses were carried out by a RIGAKU R-AXIS RAPID II imaging plate with Cu-*K*α radiation from a rotation anode source with a confocal multilayer X-ray mirror (RIGAKU VM-spider, λ = 1.54187 Å). The structures were solved by the direct method (SHELXT),[S4] and refined by the full-matrix least-squares method by applying anisotropic temperature factors for all non-hydrogen atoms using the SHELXL programs.[S5] The hydrogen atoms were placed at the geometrically calculated positions.

The crystal data of **BTICN-Hex** were summarized in Table S2. **BTICN-Hex** crystallizes in a monoclinic system with the space group $P2_1/c$, in which the half molecule is crystallographically independent. In marked difference from **BTI-Hex**, the alkyl chains are extending almost perpendicular to the core plane (Figure S3a,b). **BTICN-Hex** adopts a planar geometry and forms a uniform stacking structure with the interplanar spacing of 3.36 Å along the *b* axis (Figure S3b). The molecular overlap mode is similar to **BTI-Pr** and **BTI-Hex** rather than **BTICN-EH** (Figure S3c). Since **BTICN-Hex** has a different monoclinic space group from the *C*-centered **BTICN-EH**, all molecules in the same conducting layer are parallel to each other (Figure S3d). The molecules in the next layer are tilted oppositely (Figure S3b). There are hydrogen bonds with the distance of 2.43 Å for C≡N···H−thiophene between the adjacent columns (Figure S3d), but **BTICN-Hex** does not have any short S···S contact. Therefore, the absence of the side-by-side short S···S contact is not due to the adjacent crossing columns, but solely due to the blocking effect of the dicyanomethylene groups.

Downloaded from pubs.acs.org/aaembp/article-supplement/617211/pdf/el9b00105_si_001/ by PURDUE UNIV user on 28 October 2026

Electron transfer integrals and the calculated mobility (μ_{cal}) are listed in Table S3. Despite the absence of the S···S contact, there is a moderate intercolumnar transfer (t_a), which is comparable to the small intracolumnar transfer (t_b). The small t_b comes from the molecular overlap (Figure S3c). The resulting calculated mobility is slightly larger than **BTI-Pr** and **BTI-Hex**, which is consistent with the observations.

Downloaded from pubs.acs.org/aaembp/article-supplement/617211/pdf/el9b00105_si_001/ by PURDUE UNIV user on 28 October 2026

Table S2. Crystallographic Data of **BTICN-Hex**.

	BTICN-Hex
chemical formula	$C_{30}H_{28}N_6O_2S_2$
formula weight	568.71
crystal system	monoclinic
space group	$P2_1/c$
a (Å)	9.2227(3)
b (Å)	5.1146(2)
c (Å)	29.4199(12)
β (deg)	99.1713(18)
V (Å^3)	1369.99(9)
Z	2
total refls.	13619
unique refls. (R_{int})	2069 (0.2727)[a]
D_{calc} (g/cm^3)	1.379
R_1[b]	0.0947
R_w[c]	0.2128
GOF	0.892
T (K)	171

[a] This single crystal was extremely damaged by irradiation of X-ray, therefore R_{int} is relatively high and alert A occurred. [b] $R_1[F^2 > 2\sigma(F^2)]$. [c] $wR_2(F^2)$ for all observed reflections.

Table S3. Electron Transfer Integrals, Reorganization Energies, and Calculated Mobilities.

Compound	t_a (meV)	t_b (meV)	λ (meV)	μ_{cal} ($cm^2 V^{-1} s^{-1}$)
BTICN-Hex	20.2	−28.7	221	0.048

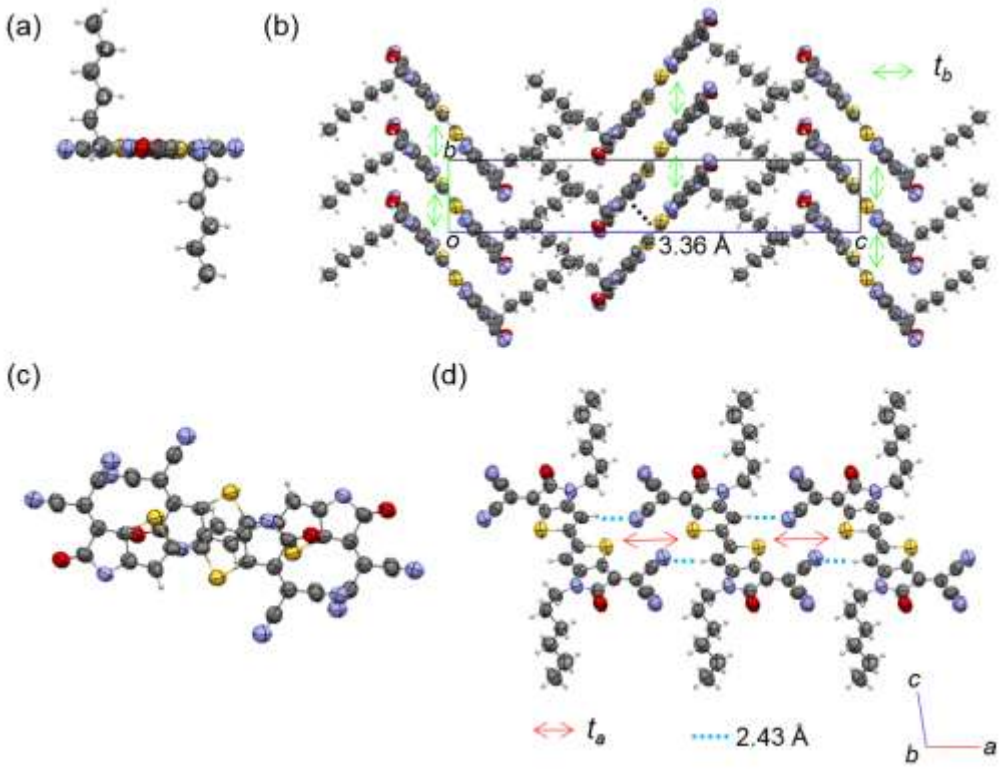

Figure S3. (a) Molecular structure of **BTICN-Hex** viewed along the molecular long axis. (b) Crystal structure viewed along the *a* axis. (c) Molecular overlap mode viewed perpendicular to the molecular plane. (d) Crystal structure viewed along the *b* axis. For clarification, the alkyl groups are omitted in (c).

Downloaded from pubs.acs.org/aaembp/article-supplement/617211/pdf/el9b00105_si_001/ by PURDUE UNIV user on 28 October 2026

V. Thin film microstructures and morphologies

The X-ray diffraction (XRD) patterns were taken by using a Philips X'Pert-Pro-MRD with CuKα radiation (λ = 1.540598 Å). Two-dimensional grazing incidence wide-angle X-ray scattering (GIWAXS) patterns were obtained at SPring-8 on beamline BL40B2.[S6] The samples were irradiated at a fixed incident angle on the order of 0.10° and the GIWAXS patterns were recorded with a 2-D image detector (PILATUS3X 2M). The wavelength of the X-ray beam was 0.1 nm (energy of 12.39 KeV) and the camera length was 341 mm.

Atomic force microscopy (AFM) images were taken by an SII scanning probe microscope system SPI3800N and SPA-300 by using a Si_3N_4 cantilever in air. AFM images of **BTI**s consist of large grains, but the grains are disconnected from each other to form non-flat surface particularly in **BTI-Pr** and **BTI-EH** (Figure S4a-c). Thin films of **BTICN**s consist of densely packed microcrystals (Figure S4d-f), and particularly **BTICN-Hex** and **BTICN-EH** form continuous large crystalline grains. Excellent transistor properties of these materials are attributed to the highly crystalline manner of the thin films.

Downloaded from pubs.acs.org/aaembp/article-supplement/617211/pdf/el9b00105_si_001/ by PURDUE UNIV user on 28 October 2026

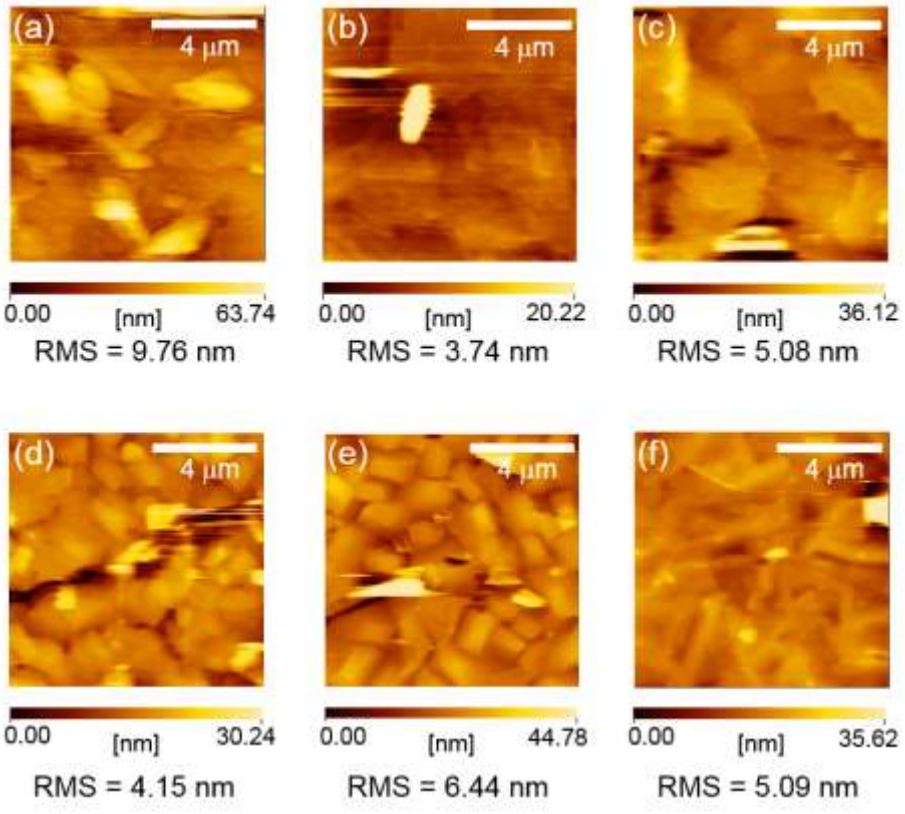

Figure S4. AFM images of (a) **BTI-Pr**, (b) **BTI-Hex**, (c) **BTI-EH**, (d) **BTICN-Pr**, (e) **BTICN-Hex**, and (f) **BTICN-EH**.

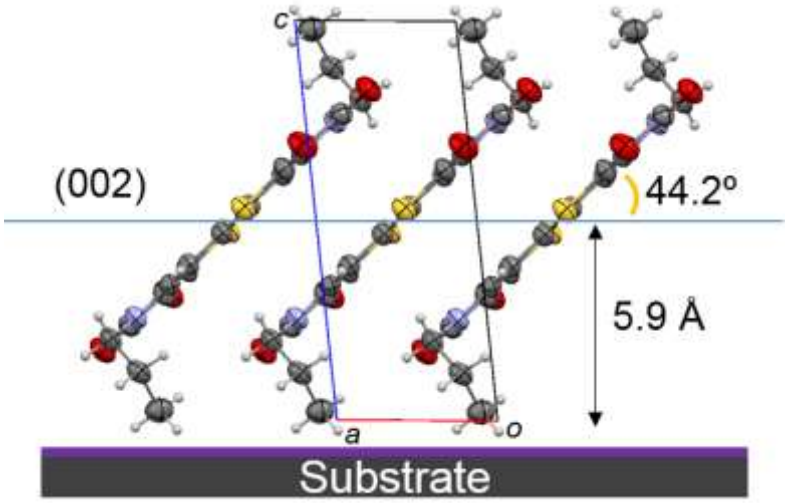

Figure S5. Molecular arrangement of **BTI-Pr** on the substrate.

Downloaded from pubs.acs.org/aaembp/article-supplement/617211/pdf/el9b00105_si_001/ by PURDUE UNIV user on 28 October 2026

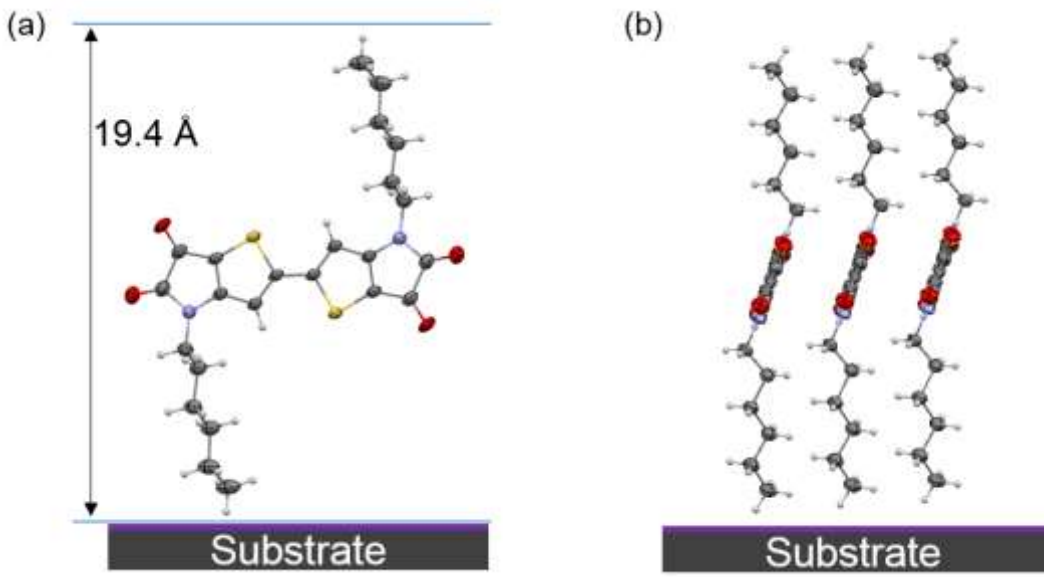

Figure S6. (a) Schematic molecular illustration of **BTI-Hex** orientation on the substrate. (b) Molecular side-on arrangement of **BTI-Hex** viewed along the molecular long axis.

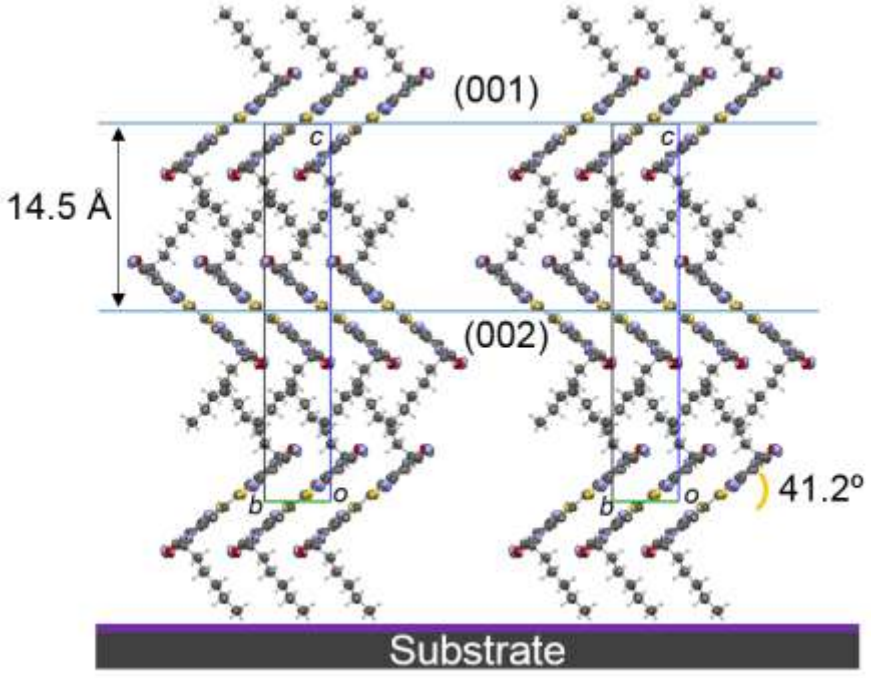

Figure S7. Molecular arrangement of **BTICN-Hex** on the substrate.

Downloaded from pubs.acs.org/aaembp/article-supplement/617211/pdf/el9b00105_si_001/ by PURDUE UNIV user on 28 October 2026

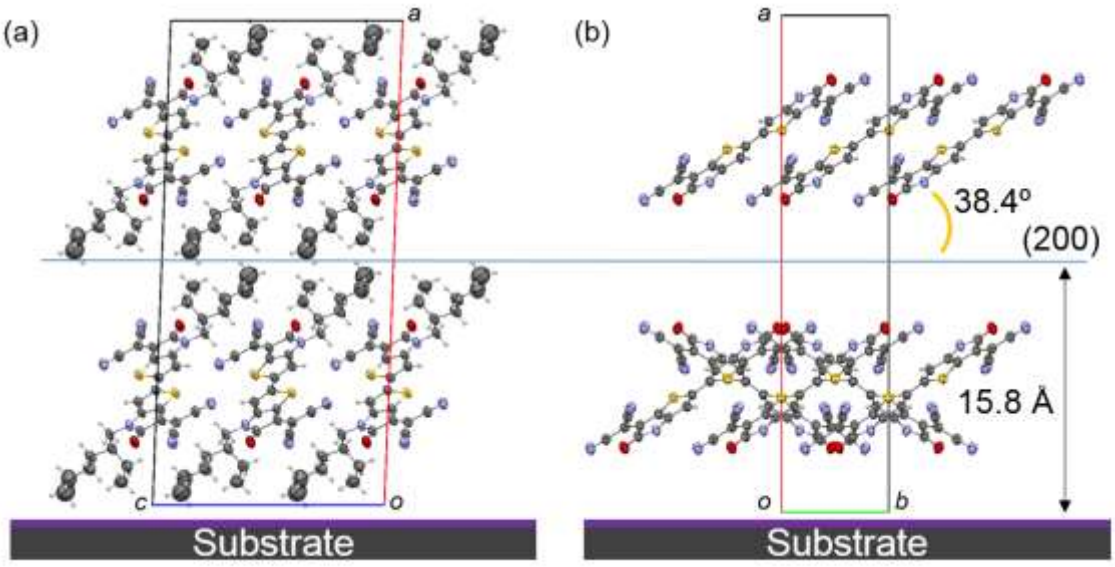

Figure S8. Molecular arrangements of **BTICN-EH** on the substrate (a) viewed along the *b* axis and (b) along the *c* axis. For clarification, the alkyl groups are omitted in (b), and another column in the upper layer is omitted in (b).

Downloaded from pubs.acs.org/aaembp/article-supplement/617211/pdf/el9b00105_si_001/ by PURDUE UNIV user on 28 October 2026

VI. Thin-film transistor properties

Output characteristics are shown in Figures S9, S10, S11, and S12. The long-term stability measurements were conducted after 150-day storage in moderate humidity (30-50%) air at room temperature (20-25°C).

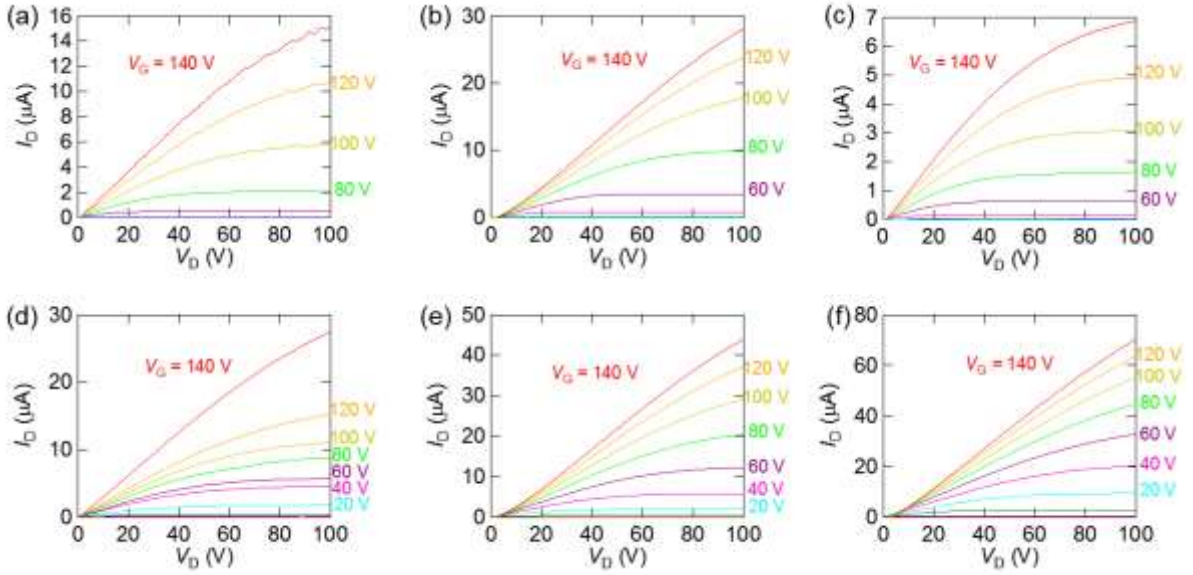

Figure S9. Output characteristics of pristine (a) **BTI-Pr**, (b) **BTI-Hex**, (c) **BTI-EH**, (d) **BTICN-Pr**, (e) **BTICN-Hex**, and (f) **BTICN-EH**, measured under vacuum.

Downloaded from pubs.acs.org/aaembp/article-supplement/617211/pdf/el9b00105_si_001/ by PURDUE UNIV user on 28 October 2026

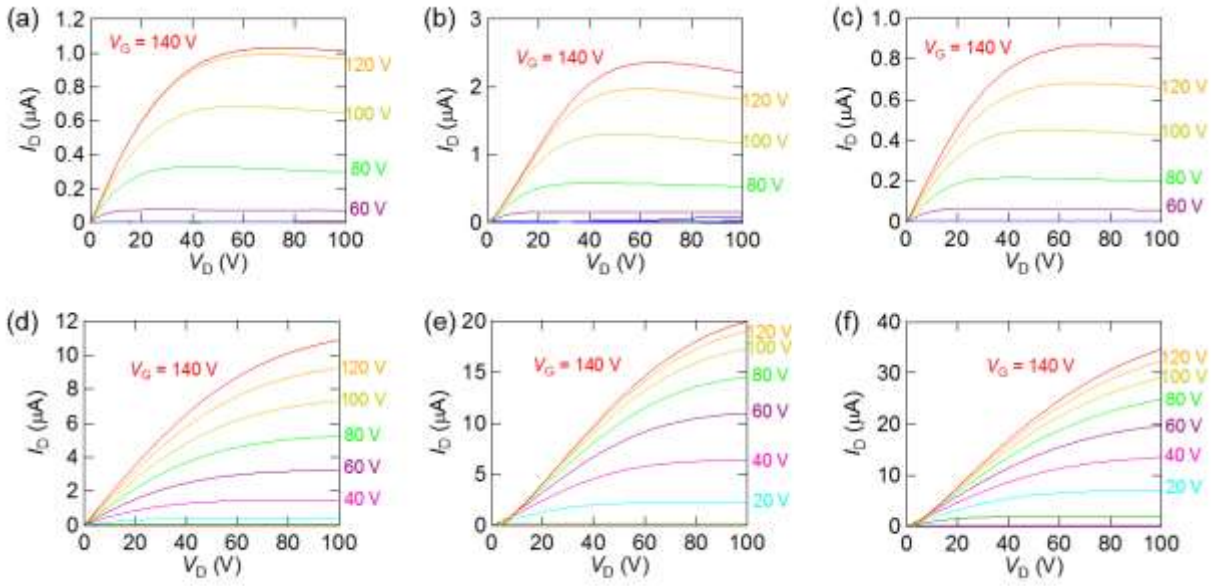

Figure S10. Output characteristics of pristine (a) **BTI-Pr**, (b) **BTI-Hex**, (c) **BTI-EH**, (d) **BTICN-Pr**, (e) **BTICN-Hex**, and (f) **BTICN-EH**, measured in air.

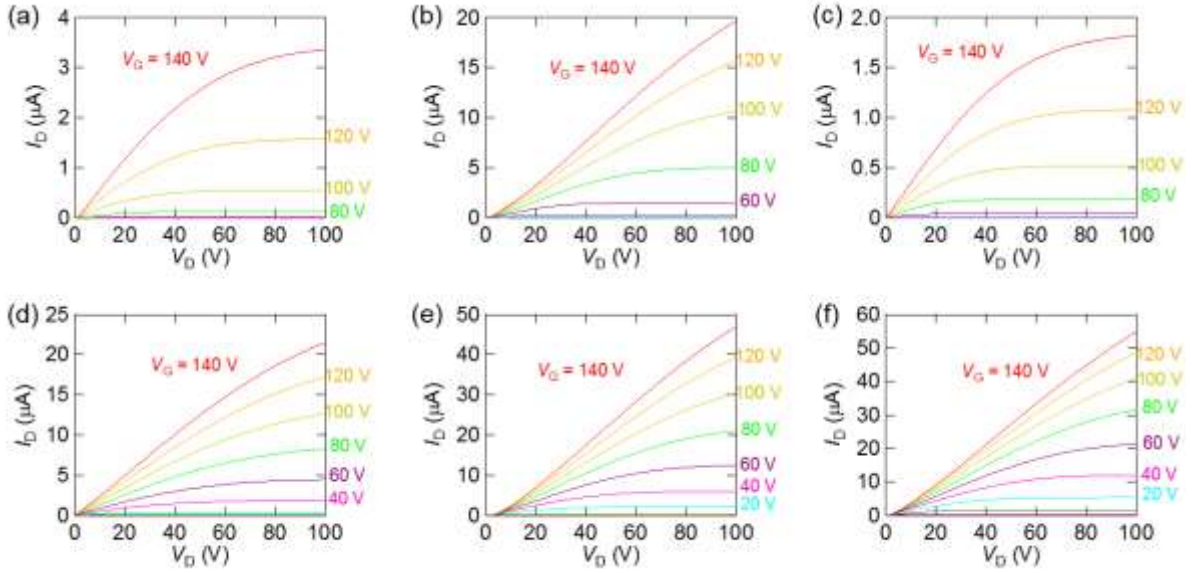

Figure S11. Output characteristics measured after 150 days under vacuum for (a) **BTI-Pr**, (b) **BTI-Hex**, (c) **BTI-EH**, (d) **BTICN-Pr**, (e) **BTICN-Hex**, and (f) **BTICN-EH**.

Downloaded from pubs.acs.org/aaembp/article-supplement/617211/pdf/el9b00105_si_001/ by PURDUE UNIV user on 28 October 2026

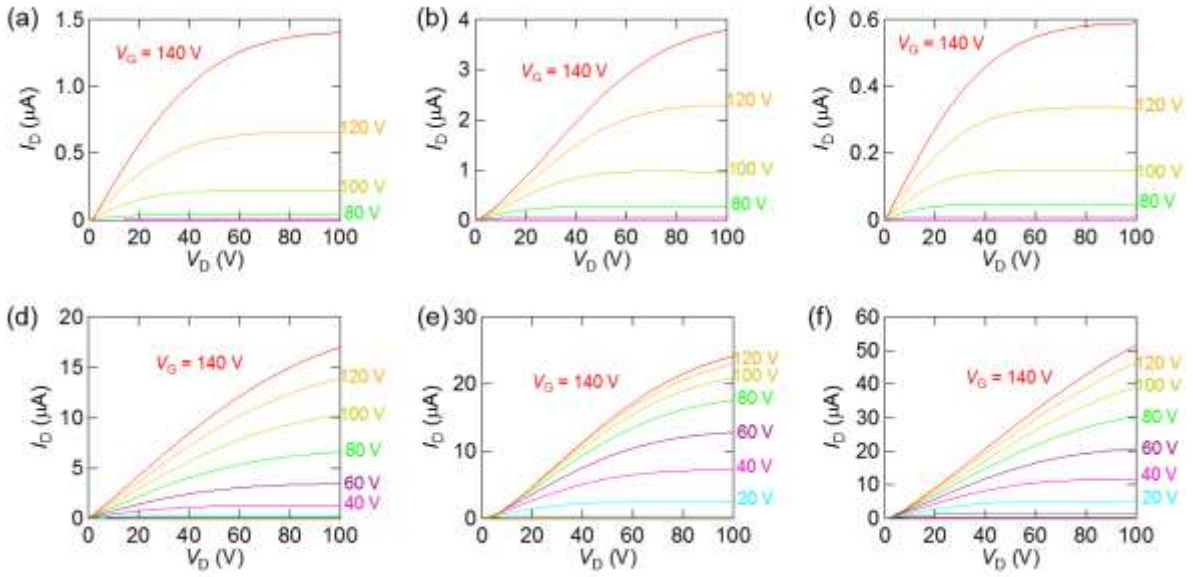

Figure S12. Output characteristics measured after 150 days in air for (a) **BTI-Pr**, (b) **BTI-Hex**, (c) **BTI-EH**, (d) **BTICN-Pr**, (e) **BTICN-Hex**, and (f) **BTICN-EH**.

Downloaded from pubs.acs.org/aaembp/article-supplement/617211/pdf/el9b00105_si_001/ by PURDUE UNIV user on 28 October 2026

REFERENCES

(S1) Van Pruissen, G. W. P.; Gholamrezaie, F.; Wienk, M. M.; Janssen, R. A. J. Synthesis and Properties of Small Band Gap Thienoisoindigo Based Conjugated Polymers. *J. Mater. Chem.* **2012**, *22*, 20387–20393.

(S2) Dasari, R. R.; Dindar, A.; Lo, C. K.; Wang, C.-Y.; Quinton, C.; Singh, S.; Barlow, S.; Fuentes-Hernandez, C.; Reynolds, J. R.; Kippelen, B.; et al. Tetracyano Isoindigo Small Molecules and Their Use in N-Channel Organic Field-Effect Transistors. *Phys. Chem. Chem. Phys.* **2014**, *16*, 19345–19350.

(S3) Pommerehne, J.; Vestweber, H.; Guss, W.; Mahrt, R. F.; Bässler, H.; Porsch, M.; Daub, J. Efficient Two Layer Leds on a Polymer Blend Basis. *Adv. Mater.* **1995**, *7*, 551–554.

(S4) Sheldrick, G. M. *SHELXT* – Integrated Space-Group and Crystal-Structure Determination. *Acta Crystallogr. Sect. A Found. Adv.* **2015**, *71*, 3–8.

(S5) Sheldrick, G. M. Crystal Structure Refinement with *SHELXL*. *Acta Crystallogr. Sect. C Struct. Chem.* **2015**, *71*, 3–8.

(S6) Fujisawa, T.; Inoue, K.; Oka, T.; Iwamoto, H.; Uruga, T.; Kumasaka, T.; Inoko, Y.; Yagi, N.; Yamamoto, M.; Ueki, T. Small-Angle X-Ray Scattering Station at the SPring-8 RIKEN Beamline. *J. Appl. Crystallogr.* **2000**, *33*, 797–800.

Downloaded from pubs.acs.org/aaembp/article-supplement/617211/pdf/el9b00105_si_001/ by PURDUE UNIV user on 28 October 2026